

## RESEARCH ARTICLE

## Cattle transport network predicts endemic and epidemic foot-and-mouth disease risk on farms in Turkey

José L. Herrera-Diestra<sup>1,2\*</sup>, Michael Tildesley<sup>3</sup>, Katriona Shea<sup>1,4</sup>, Matthew J. Ferrari<sup>1,4</sup>

**1** Department of Biology, The Pennsylvania State University, University Park, Pennsylvania, United States of America, **2** Department of Integrative Biology, The University of Texas at Austin, Austin, Texas, United States of America, **3** Zeeman Institute for Systems Biology and Infectious Disease Epidemiology Research, Mathematics Institute and School of Life Sciences, University of Warwick, Coventry, United Kingdom, **4** Center for Infectious Disease Dynamics, Pennsylvania State University, University Park, Pennsylvania, United States of America

\* [diestra@austin.utexas.edu](mailto:diestra@austin.utexas.edu)



## OPEN ACCESS

**Citation:** Herrera-Diestra JL, Tildesley M, Shea K, Ferrari MJ (2022) Cattle transport network predicts endemic and epidemic foot-and-mouth disease risk on farms in Turkey. *PLoS Comput Biol* 18(8): e1010354. <https://doi.org/10.1371/journal.pcbi.1010354>

**Editor:** Alison L. Hill, Johns Hopkins University, UNITED STATES

**Received:** August 9, 2021

**Accepted:** July 3, 2022

**Published:** August 19, 2022

**Copyright:** © 2022 Herrera-Diestra et al. This is an open access article distributed under the terms of the [Creative Commons Attribution License](https://creativecommons.org/licenses/by/4.0/), which permits unrestricted use, distribution, and reproduction in any medium, provided the original author and source are credited.

**Data Availability Statement:** The source code and data used to produce the results and analyses presented in this manuscript are available in: [10.6084/m9.figshare.20486517](https://doi.org/10.6084/m9.figshare.20486517) [10.6084/m9.figshare.20486511](https://doi.org/10.6084/m9.figshare.20486511) R code and related data to reproduce figures and analysis in the manuscript can be found in <https://github.com/jdiestra1977/ShipmentData2022.git>.

**Funding:** JLHD, KS, MF were funded by NSF-NIH-NIFA Ecology and Evolution of Infectious Disease award DEB 1911962. MT was funded by BBSRC

## Abstract

The structure of contact networks affects the likelihood of disease spread at the population scale and the risk of infection at any given node. Though this has been well characterized for both theoretical and empirical networks for the spread of epidemics on completely susceptible networks, the long-term impact of network structure on risk of infection with an endemic pathogen, where nodes can be infected more than once, has been less well characterized. Here, we analyze detailed records of the transportation of cattle among farms in Turkey to characterize the global and local attributes of the directed—weighted shipments network between 2007–2012. We then study the correlations between network properties and the likelihood of infection with, or exposure to, foot-and-mouth disease (FMD) over the same time period using recorded outbreaks. The shipments network shows a complex combination of features (local and global) that have not been previously reported in other networks of shipments; i.e. small-worldness, scale-freeness, modular structure, among others. We find that nodes that were either infected or at high risk of infection with FMD (within one link from an infected farm) had disproportionately higher degree, were more central (eigenvector centrality and coreness), and were more likely to be net recipients of shipments compared to those that were always more than 2 links away from an infected farm. High in-degree (i.e. many shipments received) was the best univariate predictor of infection. Low in-coreness (i.e. peripheral nodes) was the best univariate predictor of nodes always more than 2 links away from an infected farm. These results are robust across the three different serotypes of FMD observed in Turkey and during periods of low-endemic prevalence and high-prevalence outbreaks.

grant BB/T004312/1. The funders had no role in study design, data collection and analysis, decision to publish, or preparation of the manuscript.

**Competing interests:** The authors have declared that no competing interests exist.

## Author summary

Contact network epidemiology has been extensively used in the context of infectious diseases, primarily focusing on epidemic diseases. In this paper we use detailed recorded data about cattle exchange between farms in Turkey from 2007 to 2012, to build, analyze and characterize the directed-weighted complex network of shipments of cattle. Additionally, using outbreaks data about recorded cases of foot-and-mouth disease (FMD) in Turkey, we assess the correlation between the “farm’s” position in the network (importance) and the risk of being infected with FMD, which has been endemic in Turkey for a long time. We find some network measures that are more likely to identify high-risk and low-risk farms (in-degree and in-coreness, respectively) when proposing strategies for surveillance or containment of an infectious disease.

## Introduction

The contact structure of a population, in particular heterogeneity in the number or rate of potential contacts between individuals, is an important predictor of infectious disease transmission [1–6]. The theoretical relationship between contact structure and disease transmission dynamics has been illustrated using a variety of epidemiologically relevant contact databases [7–10]. Theory suggests that measures of contact structure are predictive of infection risk and the potential to transmit to others. Different global (eigenvector centrality, degree, coreness, betweenness) and local (random acquaintance [11]) network measures have been used to propose surveillance and vaccination strategies in static [8, 12, 13] and temporally varying [9, 14] networks. Thus, *a priori* network characterization can be used to identify candidate sites for detecting outbreaks, either in static [1, 2, 5, 15–17], temporal [18, 19], dynamic [20] or adaptive networks [21]. Moreover, these measures and their correlations are predictive of epidemic spread and can facilitate rapid targeting of interventions once an outbreak starts [22, 23]. The role of contact structure on the initial spread of infection in a naive population has been well characterized, including for the current pandemic of COVID-19 [24]. The relationship between contact structure and long-term infection risk for an endemic disease is less well characterized [25–31]. An endemic infection may experience the network topology differently from a novel outbreak [27, 32, 33], as prior infection (e.g. immunity) or interventions may alter risk and transmission of infection [34].

Livestock transportation records provide a rich resource for describing characteristics of livestock movement networks, including source location, destination, date, and batch size. Such records have been analyzed to characterize networks of interactions [35–43], and the potential consequences of network structure on the spreading of infection between farms [36, 44, 45]. However, the lack of reliable data about the infection of farms combined with detailed shipment data, has hindered our ability to build data driven models to appropriately assess the relationship between disease incidence and contact network structure in a single population, with few exceptions [46]. Instead, the impact of the interrelation between transportation network topology and disease has only been explored through theoretical simulations [13, 35, 37–40, 42, 44, 47], or through the reconstruction of who-infected-whom networks [48, 49], which describe the network of realized transmission of a specific outbreak rather than the network of potential transmission. In addition, other sources of transmission can occur through other mechanisms, including cross-border spread between premises, sharing of machinery, movement of farm workers and other forms of fomite transmission [50–54]. The development of reliable surveillance systems, both for learning about and for managing emerging or endemic

diseases remains challenging. There are many unknown characteristics of transmission and control that hamper accurate decision making, including the connectivity between farms, the duration of immunity following infection, the role of multiple serotypes circulating in the live-stock population and the use (and efficacy) of vaccines for spreading diseases, such as foot-and-mouth disease. Foot-and-mouth disease (FMD) is a highly contagious viral disease of cloven-hoofed species (such as cattle, 4, and pigs). In Turkey, FMD was eliminated in the Thrace region in 2010, but remains endemic in Anatolian Turkey. There are 7 immunologically distinct serotypes of FMD; two serotypes, A and O, have been endemic in Turkey continuously. A third serotype, Asia-1, has been present intermittently and re-emerged in Turkey in 2011 after going unrecorded since 2001.

Here, we use records of shipments of cattle (source, destination, date, batch size) among farms in Turkey to create an aggregated directed—weighted network. We first characterize the structure of the underlying network that may influence FMD spread. We then, analyze the occurrence of 3718 outbreaks of FMD in Turkey between 2007 and 2012 relative to the network defined by the livestock movement records. Over this time period, we compare the distribution of node-level measures for farms that were infected, farms at high risk (neighbors of infected farms) and farms at low risk (without neighbors that were infected), with any serotype or each serotype individually. Subsequently, by means of statistical models we quantify the relationship between node-level network measures and the odds of experiencing an outbreak. We compare the differences of these relationships between the endemic and epidemic periods of FMD, for all outbreaks (regardless of serotype) and for each serotype independently. We show that while all metrics were correlated with outbreak risk in the direction expected by theory, some metrics are significantly more correlated with either the occurrence, or absence, of outbreaks in both the endemic and epidemic phase.

## Materials and methods

### Shipment network

**The data.** The data on cattle shipments was provided by the Turkish Veterinary authorities, facilitated by the European Commission for foot-and-mouth disease (EuFMD), who granted the access to data from the TurkVet database. The highest resolution of cattle farming unit in Turkey is the holding, of which there are over 2.9 million. In each holding, birth, movement, and death data are recorded. The number of animals on these holdings can range from fewer than 5 to over 500. Since many of these holdings are small, the basic epidemiological unit for recording FMD outbreaks in Turkey is the epiunit (a village or a neighbourhood comprised of several holdings [55]); there were 49850 epiunits in Turkey (Fig 1a) after aggregation. The data did not identify which epiunits were markets or abattoirs, and therefore all epiunits were treated as similar. (A more detailed description in Tables A and B, Section A in S1 Appendix).

**Network construction.** We created the livestock movement (shipments) network, where each epiunit is represented by a node, and an edge is placed between two epiunits if there existed a shipment of cattle between them. In general, a graph  $G$  can be defined as a pair  $(V, E)$ , where  $V$  is a set of vertices, and  $E$  is a set of edges between the vertices  $E \subseteq (u, v) | u, v \in V$ . A graph or network can be represented as an adjacency matrix  $A$ , defined as

$$A = \begin{cases} A_{ij} = w_{ij} & \text{if } i \text{ is connected to } j \\ 0 & \text{otherwise.} \end{cases} \quad (1)$$

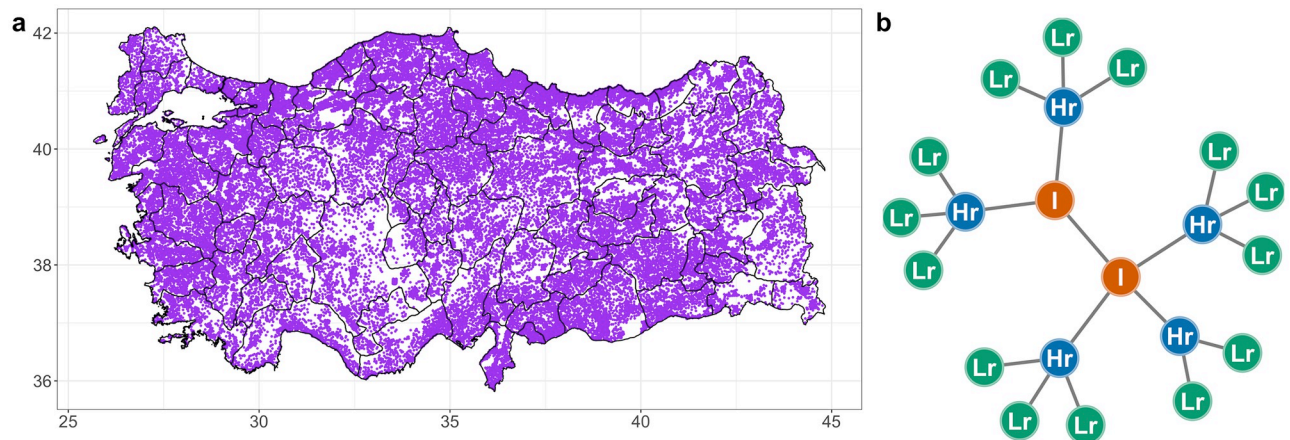


**Fig 1. Location of epiunits in Turkey.** Each purple dot represents the location of an epiunit in the map. **b.** Schematic representation for the definition infectious state of epiunits: Infected (red); high-risk (blue) and low-risk (green). Base layer of map available from [https://gadm.org/download\\_country.html](https://gadm.org/download_country.html) with license <https://gadm.org/license.html>.

<https://doi.org/10.1371/journal.pcbi.1010354.g001>

The network considered here is an aggregation of all shipments between epiunits, which created a static—aggregated network (from here on called the shipments network). The shipments network is directed (there is information about origin—destination of shipments) and weighted; the weights,  $w_{ij}$ , are calculated using the frequency of unique shipments, regardless of the number of animals in the shipment, between epiunits, due to the fast-spreading nature of FMD within premises [56].

## Network description

Among the many of statistics used to characterize a complex network, we focused on those that have been used in previous studies and shown to be related to spreading dynamics; particularly epidemics [38, 42, 44, 57–65]. Further details about each of these measures in Section B in [S1 Appendix](#).

We calculated the following global measures, which summarized properties over all nodes: density ( $d$ ), average shortest path length ( $L$ ); diameter ( $D$ ); degree assortativity ( $\rho$ ); giant strongly connected components ( $GSCC$ ); giant weakly connected components ( $GWCC$ ); largest eigenvalue of the adjacency matrix ( $\lambda_1$ ); reciprocity ( $r$ ); the global clustering coefficient ( $C$ ); and modularity ( $Q$ ) using the Louvain community detection algorithm [66, 67]. We compared the global attributes of our network with an ensemble of 100 random equivalent networks as null models [68] using the Z-score of each measure. Due to the large size of the shipments network and computational limitations, the calculation of  $L$  and  $D$  were performed in the directed—unweighted version of the network (lower bound); while  $C$  and  $Q$  were calculated on the undirected—weighted version of the network which gives an upper bound [57, 69, 70].

Additionally, we calculated local (node-level) measures, which describe the characteristics of each epiunit in the network: in/out degree ( $k_i^{in/out}$ ); in/out strength ( $s_i^{in/out}$ ); in/out  $k$ -coreness ( $kC_i^{in/out}$ ) and eigenvector centrality ( $ec(i)$ ) (we also calculated the relative betweenness centrality ( $B_i$ ) in Section D to Section F in [S1 Appendix](#)—which did not present significant differences with the measures shown here). In each measure  $i$  refers to epiunits and in/out refers to the direction of the shipments used to calculate the measure.

Furthermore, for all measures with in and out modes (degree, coreness, strength), we introduced a simple measure that compares the balance between in and out shipments for each epiunit. We defined the “transmission flux” ( $\phi$ ) of epiunit  $i$  as

$$\phi_{X \in \{\text{degree, strength, coreness}\}}^i = \frac{X_{in}^i - X_{out}^i}{X_{in}^i + X_{out}^i}, \quad (2)$$

where  $X \in \{\text{degree, strength, coreness}\}$  are measures that were calculated using in and out modes. Note that  $\phi_X^i \in [-1, 1]$ . When an epiunit  $i$  has  $\phi_X^i = -1$ ,  $X_{in} = 0$  and  $X_{out} \neq 0$ , it is a net “source” of shipments. A value of  $\phi_X^i = 1$ ,  $X_{out} = 0$  and  $X_{in} \neq 0$ , identifies net “sink” epiunits. An epiunit  $i$  with  $\phi_X^i = 0$  and  $X_{in}, X_{out} \neq 0$ , interacts with its neighborhood reciprocally ( $X_{in} = X_{out}$ ). Our transmission flux ( $\phi_X^i$ ) discriminates between epiunits according to their vulnerability to get infected from a spreading disease (sinks) and their ability to transmit infection (sources) [23].

Lastly, we compared our shipments network with conventional well studied networks, calculating the Spearman correlation between the matrices of correlation of node-level measures. All calculations were performed in R, and those related to complex networks statistics with the R package igraph [71].

### FMD spreading in Turkey

In addition to the data of shipments between epiunits, 6112 outbreaks of FMD (with identified serotypes) were reported to TurkVet between January 2001 and July 2012. The data included epiunits’ locations and dates of detected outbreaks. We focused our analysis to the period of time which overlapped with the shipments data (from 2007 to 2012), which included 3718 outbreaks. Our study assumes transmission due to exchange of shipments; however, transmission can occur through other mechanisms, i.e. cross-border spread between premises, sharing of machinery, movement of farm workers, and other forms of fomite transmission [50–54]. Here, these additional sources of transmission would be attributed to background risk of infection.

We first compared the distribution of local network measures for nodes that experienced outbreaks to those that did not. Then we estimated the relative effect of local measures on the odds of experiencing outbreak. We repeated these steps for all serotypes in combination and for each serotype independently.

**Descriptive analysis of outbreak risk.** For each epiunit in the shipments network we assigned the following state labels (Fig 1b):

1. Infected epiunits (I) (red); epiunits that experienced at least one outbreak of FMD.
2. High-risk epiunits (Hr) (blue); epiunits that were directly connected (through at least one shipment) to an epiunit that experienced a FMD outbreak.
3. Low-risk epiunits (Lr) (green); epiunits that were at least at distance two (two degrees of separation) from an infected epiunit.

We then compared the distribution of local network measures of each epiunit as a function of these states, by creating several correlation planes of node-level features.

**Statistical models of outbreak risk.** To estimate the relative correlation between local network measures and outbreak risk we fitted univariate logistic regressions for each variable of interest (coreness, degree, strength, transmission flux of degree and coreness, and eigenvector centrality), in addition to a multivariate model including all these variables. We dichotomized the node states into infected nodes = 1 and all others = 0 (as defined above), to estimate



the odds of infection associated with each local measure independently (univariate models) and collectively (multivariate model). Similarly we repeated these analysis with the node state dichotomized into low-risk epiunits = 1 and all others = 0 to estimate the odds of avoiding exposure associated with each local measure. Due to the high degree of skewness of the local network measures we log-transformed each of them (Fig A in Section G of [S1 Appendix](#)). We fitted these models to different temporal epochs within the time series (Table A in Section G of [S1 Appendix](#)); for each period we recalculated local network measures for the network of shipments and used the infection status during that period. Specifically, considering all outbreaks regardless of serotype, we considered the “complete” time series of all FMD outbreaks between 2007–2012; the “endemic” period, defined as before 15 February 2010 (moment when the number of outbreaks exceeded their average number for more than four consecutive days); the “epidemic” period, after 15 February 2010. Because there were many more outbreaks during the epidemic period we also considered an “epi-partial” period defined as the time period that contains all outbreaks from 15 February 2010 until the total number of outbreaks in the epi-partial period was equal than that of the total number of infected epiunits in the endemic regions (19 September 2010).

We then repeated the above for serotypes O and A independently, defining each epoch accordingly (Table A and Fig B in Section G of [S1 Appendix](#)). Using the aggregated shipments within each period defined above, we built directed-weighted networks and calculated node-level measures for each epiunit and fitted logistic regressions to the epidemic state of the node during each defined epoch. For serotype Asia-1 we considered all time points when outbreaks were present as epidemic. We classified and selected models according to the Bayesian Information Criteria (BIC).

## Results

### Characterization of the shipments network

The shipments network is a directed-weighted network which consists of  $N = 49,580$  nodes (epiunits) that are connected with  $E = 4,746,035$  edges. The shipments network is a “complex network”; it shows a combination of features that are significantly different from random equivalent networks which are shown by the Z-scores calculated for each global measure ([Table 1](#)—Complete set of measures [Table A](#) in Section B of [S1 Appendix](#)).

Specifically, the shipments network shows strong evidence of small-worldness (large clustering coefficient and small shortest path length), along with a diameter that covers the complete network in 20 steps; as well as a strong modular structure ( $Q = 0.67$ ) (much larger than expected for a random network). There were  $\approx 110$  modules with more than 10 epiunits. ([Table 1](#)). The exchange of cattle occurs at many scales (Fig A in Section B of [S1 Appendix](#))

**Table 1. Network measures for the shipments network** (\*Calculated using the directed-unweighted version of the network. \*\*Calculated using the undirected-weighted version of the network).

Measure	Value	Z-score
Shortest path length ( $L$ )	2.86*	0.01
Diameter ( $D$ )	20*	0.32
GSCC	97%	-
GWCC	100%	-
Largest eigenvalue ( $\lambda_1$ )	3280.40	195.03
Clustering coeff. ( $C$ )	0.51**	23.69
Modularity( $Q$ )	0.67**	1540.97

<https://doi.org/10.1371/journal.pcbi.1010354.t001>

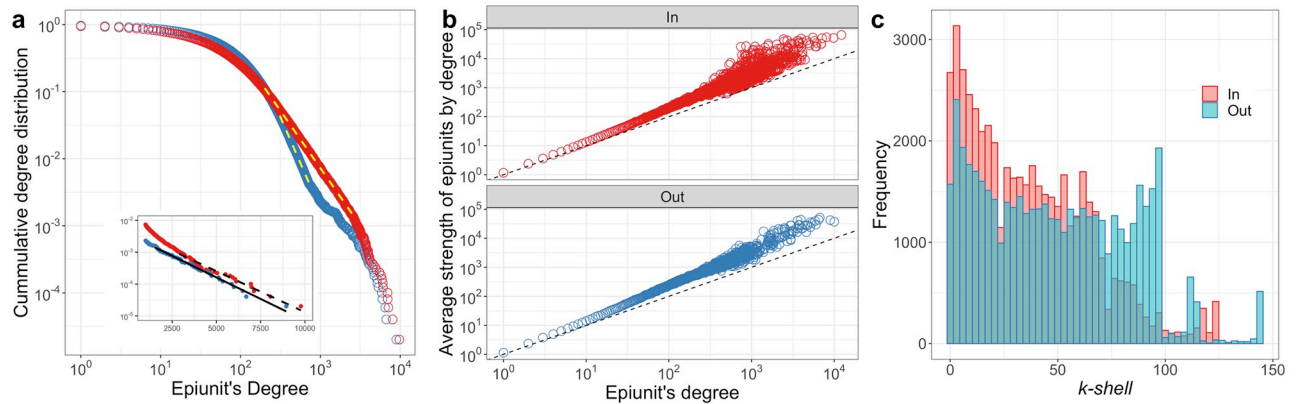


**Fig 2.** a. Log-Log plot of the complement of the cumulative distribution of in (red) and out (blue) degrees. Yellow dashed lines show the scale-free region of in/out degree. The inset shows the exponential decay of the tail for both distributions and the exponential fit. b. Average strength  $\bar{s}(k)$  of epiunits with degree  $k$  for in/out degree/strength, as indicated in panels. Dashed line indicates  $s_i = k_i$ . c. Frequency of epiunits in each (in—red/out—blue)  $k$ -shell in the network.

<https://doi.org/10.1371/journal.pcbi.1010354.g002>

with a typical distance around 5 km and few long distance shipments ( $\sim 120$  km) that connect otherwise geographically separated regions.

The degree distribution of the shipments network is strongly right-skewed. It is best-fit by a log-normal distribution (Tables A and B and Fig A in Section C of [S1 Appendix](#)), but illustrates scale-free behavior for nodes of intermediate degree (Fig 2a—yellow dashed lines) and an exponential cut-off for nodes with large degree (Fig 2a and inset) [72]. The strength of each edge (i.e. the number of shipments to (in-strength) and from (out-strength) each epiunit) is strongly correlated with degree but grows faster than degree, implying that high degree nodes also receive disproportionately more frequent shipments (Fig 2b). The nucleus [59] of the shipments network (all epiunits in the highest  $k$ -shell; i.e. largest coreness) is formed by 0.8% and 0.9% of all epiunits for the in and out coreness, respectively (Fig 2c). Together, the high degree of variability in node-level measures suggests that we should see highly heterogeneous outbreak risk.

Lastly, after removing all epiunits ever infected from the shipment network, along with their connections, the GSCC of the residual network is 0.96; thus, 96% of epiunits in the residual network can be reached from any other epiunit through directed connections. A full description of the features of the network and comparison to other families of network models is presented in Section D in [S1 Appendix](#).

### FMD outbreaks in Turkey

Serotypes O and A were present in Turkey throughout 2001–2012, with large outbreaks in 2006 and 2011 (serotype A) and 2007 and 2010 (serotype O). Additionally, there were two incursions of serotype Asia-1 in 2001 and 2012. (Fig 3a). The serotypes A and O were present across all Turkey, while the serotype Asia-1 outbreaks were disproportionately concentrated in the west of the country (Fig 3b).

Of all 49,580 epiunits in the shipments network, 3437 were involved in at least one outbreak of any serotype between January, 2007 to July, 2012. Serotype O was detected in 1637 epiunits, 1356 epiunits were infected with serotype A, and 444 epiunits infected with serotype Asia-1. Most epiunits experienced only 1 outbreak of any serotype; though 1 epiunit had 8 outbreaks of serotype A, 1 epiunit had 5 outbreaks of serotype O, and one epiunit had 3 outbreaks of serotype Asia-1. Of all epiunits, 19 experienced outbreaks of all three serotypes.

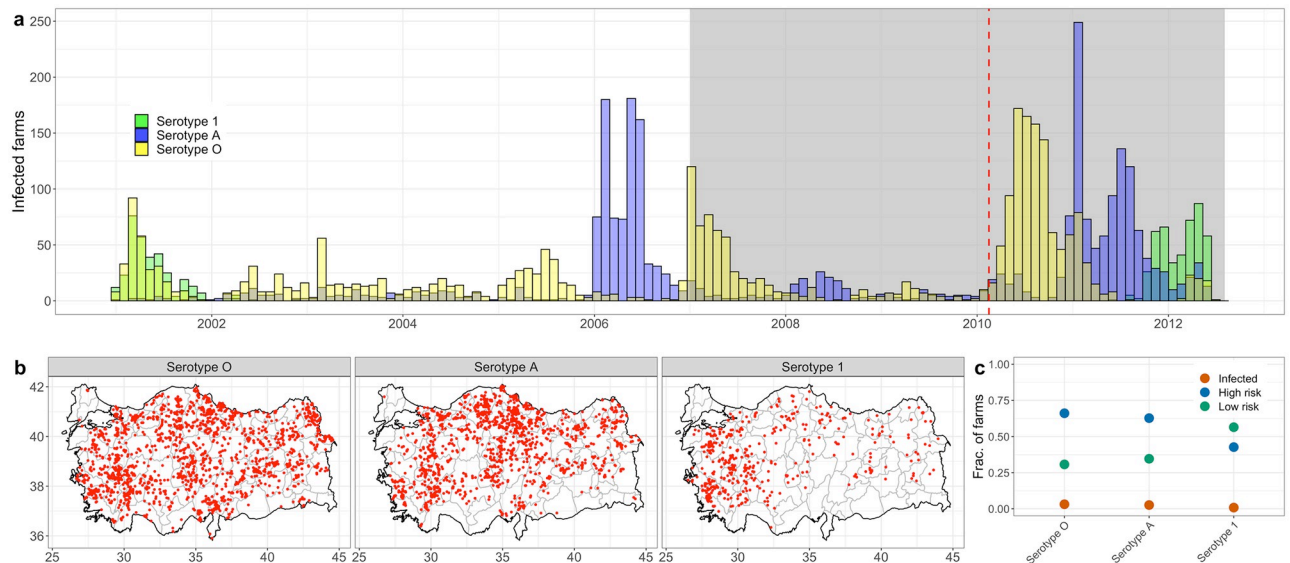


**Fig 3. a.** Incidence (accumulated by month) of each strain of FMD in Turkey. The gray region shows the time range where the outbreak data and the shipments data overlap (2007–2012). The red dashed vertical line delineates the endemic (left) and epidemic (right) regions, regardless of serotype, at February 15, 2010. **b.** Maps of Turkey showing the location of each of the epiunits (red points) where there occurred an outbreak of FMD. Each panel shows the location of epiunits where occurred at least one outbreak, according to serotype. **c.** Fraction of epiunits in each state (infected (red), High risk (blue) and Low risk (green), for each FMD serotype. Base layer of maps available from [https://gadm.org/download\\_country.html](https://gadm.org/download_country.html) with license <https://gadm.org/license.html>.

<https://doi.org/10.1371/journal.pcbi.1010354.g003>

Infected nodes were disproportionately central to the network, and low-risk nodes were disproportionately peripheral. Epiunits infected by serotypes O and A accounted for  $\approx 10\%$  of the total sum of normalized centrality (the sum of the ratio between the centrality of each epiunit and the total sum of centrality in the network; Fig A in Section E of [S1 Appendix](#)) of the shipments network regardless of the measure, despite being 3.2%, 2.6% of all nodes, respectively (Fig 3c). In contrast, epiunits infected with the Asia-1 serotype (0.8% of all epiunits; Fig 3c) comprise approximately 1% of total sum of normalized centrality. Low-risk epiunits are under-represented with respect to network centrality. For serotypes O and A, low-risk epiunits accounted for  $\approx 30\%$  of all epiunits (Fig 3c); these epiunits reflect  $\approx 0.1\%$  of eigenvector centrality and  $\approx 10\%$  out-coreness centrality, implying that these epiunits are disproportionately on the periphery of the shipments network. Epiunits that were low-risk with respect to the Asia-1 serotype were also disproportionately non-central in the shipments network, though less so than the O and A serotypes (Fig A in Section E of [S1 Appendix](#)).

**Descriptive analysis of outbreak risk.** For all serotypes, there is a positive correlation between in-degree ( $k_i^m$ ) and eigenvector centrality ( $ec$ ; Fig 4a; correlation value considering all epiunits, regardless of infectious state 0.69). Low-risk epiunits had disproportionately lower in-degree ( $k_i^m$ ) and eigenvector centrality ( $ec$ ) than infected epiunits, with nearly all low-risk epiunits below the mean value for both measures (Fig 4a). Infected epiunits had a similar distribution of in-degree and eigenvector centrality as high-risk (neighbors of infected) epiunits for serotypes O and A (Fig 4 marginal plots). Epiunits infected with serotype Asia-1 tend to have higher eigenvector centrality than the mean for the network. In-coreness (Fig 4b) was positively correlated with eigenvector centrality. Low- and high-risk epiunits occur across the range of values of in-coreness; but, low-risk epiunits disproportionately had low values of in-coreness. Infected epiunits had disproportionately high values of in-coreness. Thus infection with all three serotypes was more likely in the nucleus of the network. The flux in degree and



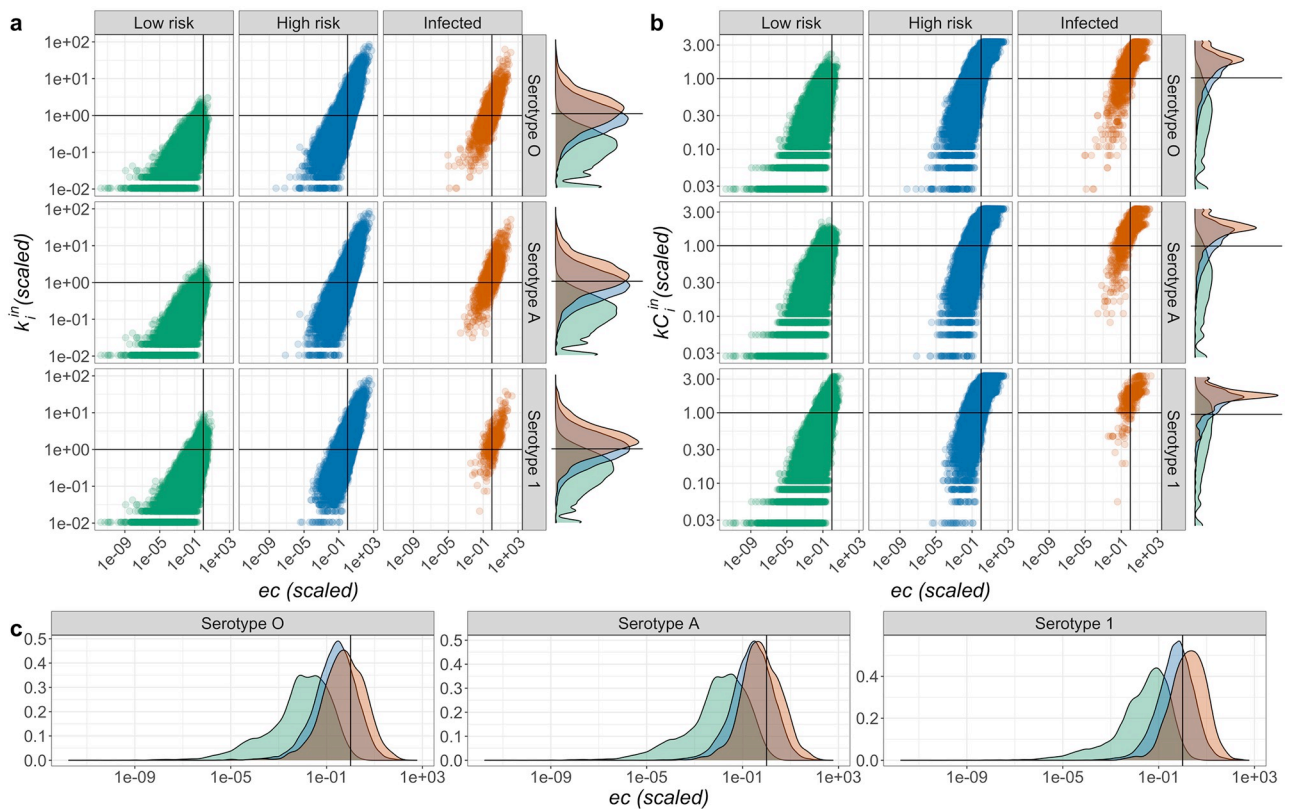


**Fig 4. Correlation planes for different network measures of epiunits, by infectious state; i.e. eigenvector centrality ( $ec$ ), in-degree ( $k_i^{in}$ ), in-coreness ( $kC_i^{in}$ ).** a. Correlation plane ( $ec, k_i^{in}$ ). Marginal plots correspond to densities of  $k_i^{in}$ . b. Correlation plane ( $ec, kC_i^{in}$ ). Marginal plot corresponds to the densities of  $kC_i^{in}$ . c. Density plots for  $ec$  for each of the three serotypes.  $k_i^{in}$ ,  $kC_i^{in}$  and  $ec$  have been re-scaled using their corresponding mean value in the complete network. Horizontal lines show, for  $k_i^{in}$  and  $kC_i^{in}$ , the mean value for reference. In all panels colors correspond to low-risk (green), high-risk (blue), and infected (red) epiunits for each of the three serotypes (rows) (a and b). Vertical lines show the location of the mean value for the  $ec$  in all plots. Different strains of FMD are as labeled.

<https://doi.org/10.1371/journal.pcbi.1010354.g004>

coreness was neither correlated with  $ec$  (0.12 and 0.06, respectively), nor different among node states (Fig A in Section F of S1 Appendix).

**Statistical models of outbreak risk.** The odds of being infected (with any serotype) was significantly positively correlated ( $OR > 1$ , Fig 5a) with all node level measures for the complete time series and in all 3 subset periods (endemic, epidemic and epi-partial). Similarly, the odds of being a low-risk node (greater than 1 edge from an infected node) was significantly negatively correlated with all measures. In-degree was the best fit among univariate models (determined by BIC) for predicting epiunits with an infected state (Fig 5a). The best predictor of low-risk state (given by lowest BIC) was the in-coreness (Fig 5b).

For a multivariate model including all variables, in-degree is the only variable that is consistently significant and positively correlated with infection of epiunits in all epochs (Fig 5c). Both in-degree and in-coreness are significant and negatively correlated with low-risk epiunits (Fig 5d). These results hold when considering independent serotypes and the different regions (Fig C in Section G of S1 Appendix).

## Discussion

Here we used a large and detailed database of cattle shipments between epiunits in Turkey, to build and characterize an aggregated directed-weighted network. Over a 6 year period from

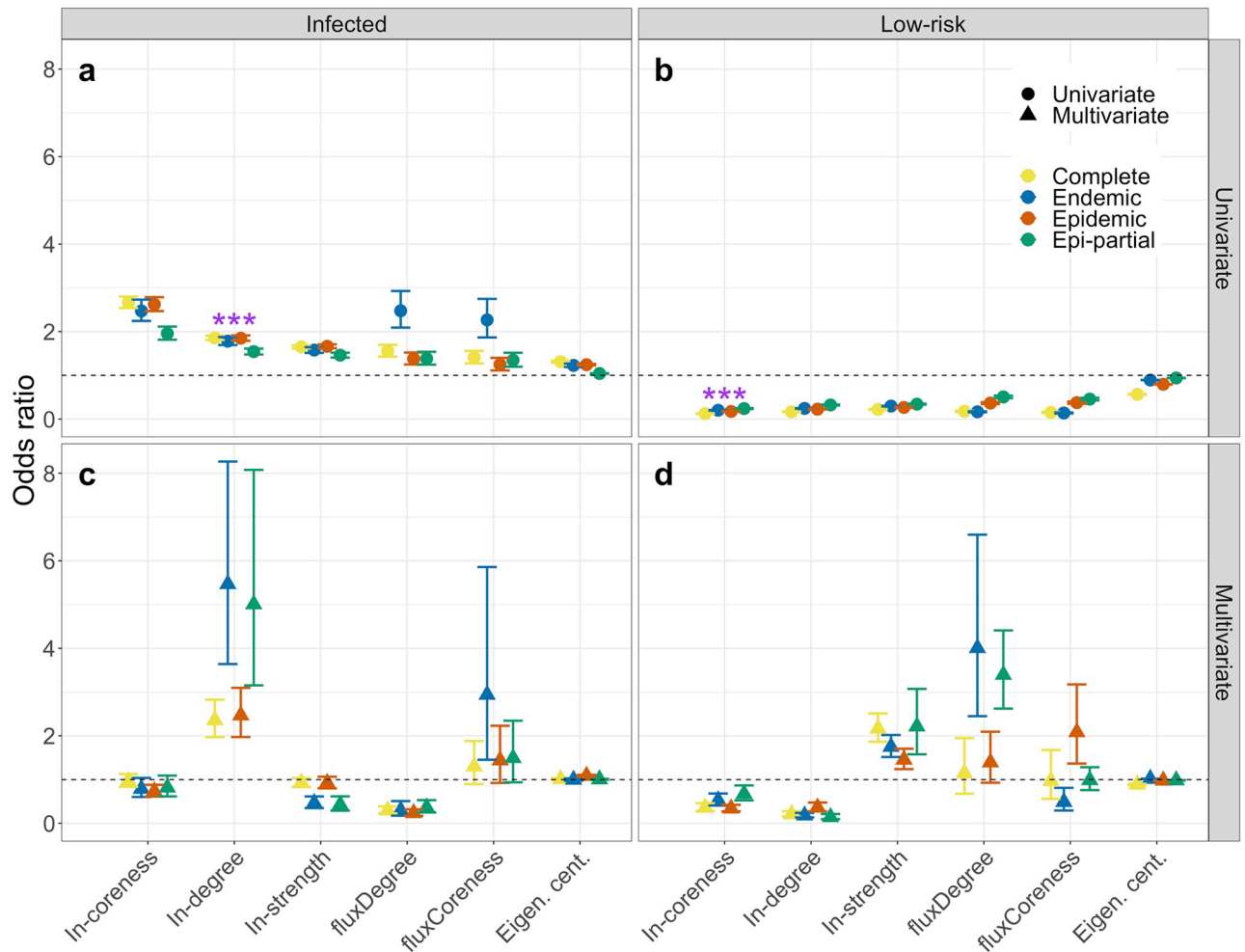


**Fig 5.** a and b) and multivariate (c and d) models. Complete network, aggregated in the corresponding period considered (2007–2012), endemic region (before February 15, 2010, epidemic region (after February 15, 2010), and epi-partial, (after February 15, 2010, until the aggregated number of outbreaks is similar to the number of outbreaks in the whole endemic region). The best univariate predictor (based on BIC) is indicated with “\*\*\*\*” in panels (a and b). Results for each independent serotype in Section G in S1 Appendix.

<https://doi.org/10.1371/journal.pcbi.1010354.g005>

2007–2012 the occurrence of FMD outbreaks in Turkey were correlated with node-level network characteristics. Specifically, using univariate models, in-degree (i.e. receiving many shipments) was the variable with the best fit when predicting outbreaks, while epiunits with low in-coreness (nodes on the periphery of the network) were better predicted to have low risk. These behaviors hold when considering multivariate models (in-degree is in the correct direction of association when predicting the odds of having an outbreak; and in-coreness is also still predictive of low-risk epiunits), nonetheless, the individual contribution of each variable has an unexpected behavior. Notably, these results are consistent regardless of serotype and of the different periods considered (complete, endemic, epidemic, epi-partial).

The Turkey shipments network is complex, with a combination of global measures that has not been reported for other similar networks [38, 39]. The directed nature of the network is given by the identification of origin-destination epiunits; and the weight of each edge is given by the frequency of shipments between epiunits, due to the fast-spreading nature of FMD within premises [56]. The shipments network is small-world (small shortest path length, and large clustering coefficient), also showing that in an ideal case, an infectious disease

could reach a large fraction of the epiunits ( $GSCC = 97\%$ ) in a small number of generations ( $D = 20$ ) [3].

Notably, even after removing all epiunits that experienced outbreaks and their connections, the  $GSCC$  of the residual network remains high (96%), a property shared among scale-free-like networks (robust under random failure), which at the same time makes them vulnerable to intentional and targeted attacks [1]. Consequently, the relatively limited penetration of FMD into the shipments network may reflect the effect of local mitigation efforts (e.g. reactive vaccination and movement controls) and structural elements of the network itself. In particular, we find that the network is highly modular  $Q = 0.67$ ; such modularity has been shown to reduce the risk of large outbreaks [73, 74]. It is important to mention that one limitation of our data is the lack of distinction of epiunits; i.e. regular epiunits, markets or abattoirs. This may potentially underestimate transmission risk [53]; however, we are not able to estimate the scale of this underestimation. Despite this, we believe that our analysis provides strong evidence of the risk associated with transmission through the livestock network. We note that our flux measures *could* identify the importance of nodes that are strong “sinks” of shipments, such as abattoirs. Flux in degree and coreness did have large effect size for association with infection in the endemic epochs, but were not the best fit univariate measure and reversed direction. Additionally, even when other mechanisms of transmission may be in play (cross-border spread between premises, sharing of machinery, movement of farm workers, and other forms of fomite transmission) we only focused on the transmission that may occur due to the exchange of shipments [50–54].

Though FMD outbreaks between 2007–2012 were broadly distributed across the country (Fig 3b), there were distinct relationships between node-level network properties and the likelihood of an epiunit experiencing an outbreak; or, conversely that an epiunit was at low-risk for exposure to an FMD outbreak. Primarily, considering each metric independently, epiunits that recorded outbreaks (of any serotype) had disproportionately higher in-coreness and in-degree, were more likely to be net recipients of shipments, and had higher eigenvector centrality compared to epiunits that never recorded an outbreak; and the converse was true for epiunits that were greater than 1 edge away from outbreaks (Fig 4). Among all univariate models, in-degree was the best predictor of infection in the network (Fig 5a); the more shipments received by an epiunit, the more risk of infection. On the other hand, even when all univariate models predicted that low-risk epiunits would have the lowest scores regardless of the node-level measure used, in-coreness was the best predictor of epiunits that were safe from an ongoing outbreak (Fig 5b).

The univariate correlations were robust both across serotypes and during low and high prevalence periods in the time series. This observation is important as it implies a broad consistency in dynamics of exposure outbreaks. Further, analysis of risk during low-prevalence, endemic periods (e.g. 2008–2010) would give qualitatively similar assessment of the risk of outbreak (similar odds ratio) as would be expected during high-prevalence outbreaks. Similarly, analysis of any one serotype (or all serotypes combined) would give a similar assessment of risk as for any individual serotype; e.g. the re-emergence of the Asia-1 serotype in 2011 (Section G in S1 Appendix).

It is customary that strategies for surveillance and control in networks are implemented using individual network measures [8–12, 75–79]. Combining measures to better identify high-risk epiunits seems a reasonable avenue. However, we found that a multivariate model led to counter-intuitive effects. The best univariate predictors remained significant and in the expected direction in the multivariate model, but the coefficients on many of the other predictors switched direction (Fig 5c and 5d). We note that there is high correlation among the node-level measures themselves (Fig A in Section D of S1 Appendix) and their interactions

with respect to outbreak risk are unlikely to be simple or linear. The intricacies of the appropriate combination of measures in a multivariate model is an interesting avenue for further study.

Our results suggest that a plausible strategy for the placement of sensors for surveillance in the network could be applied in two sequential steps: given the complex network (1) calculate the in-coreness of the network and discard all nodes in the periphery of the network; (2) in the residual network, select an appropriate fraction  $f$  of the best ranked nodes according to in-degree. Furthermore, our results show that in the shipment network discarding epiunits with low in-coreness could be a potential criteria for vaccination campaigns (path to optimal allocation of resources); while the in-degree could be used to identify epiunits with high spreading impact in an ongoing outbreak (placement of sensors for surveillance).

The analysis of the aggregated shipments network opens questions which can be approached in future research. For instance, the robustness of epiunits' importance using a temporal network approach [80]. Additionally, the possibility of implementing, proposing and evaluating current and novel strategies for control and surveillance of infectious diseases.

## Supporting information

**S1 Appendix. Supplemental material.** File containing supplementary explanation and additional tables and figures to complement results shown.  
(DOCX)

## Author Contributions

**Conceptualization:** José L. Herrera-Diestra, Matthew J. Ferrari.

**Data curation:** José L. Herrera-Diestra.

**Formal analysis:** José L. Herrera-Diestra.

**Funding acquisition:** Michael Tildesley, Katriona Shea, Matthew J. Ferrari.

**Investigation:** José L. Herrera-Diestra.

**Methodology:** José L. Herrera-Diestra.

**Project administration:** Michael Tildesley, Katriona Shea, Matthew J. Ferrari.

**Software:** José L. Herrera-Diestra.

**Supervision:** Matthew J. Ferrari.

**Validation:** José L. Herrera-Diestra.

**Visualization:** José L. Herrera-Diestra.

**Writing – original draft:** José L. Herrera-Diestra, Matthew J. Ferrari.

**Writing – review & editing:** Michael Tildesley, Katriona Shea, Matthew J. Ferrari.

## References

1. Albert R, Jeong H, Barabási AL (2000) Error and attack tolerance of complex networks. *Nature*, 406:378–382. <https://doi.org/10.1038/35019019> PMID: 10935628
2. Watts D, Strogatz S (1998) Collective dynamics of 'small-world' networks. *Nature*, 393:440–442, <https://doi.org/10.1038/30918> PMID: 9623998
3. Newman MEJ (2003) Properties of highly clustered networks. *Phys. Rev. E*, 68:026121, <https://link.aps.org/doi/10.1103/PhysRevE.68.026121> PMID: 14525063

4. Eubank S, Guclu H, Kumar VSA, Marathe MV, Srinivasan A, Toroczkai Z, et al. (2004) Modelling disease outbreaks in realistic urban social networks. *Nature*, 429:180–184, <https://doi.org/10.1038/nature02541> PMID: 15141212
5. Meyers LA, Pourbohloul B, Newman MEJ, Skowronski DM, Brunham RC (2005) Network theory and SARS: predicting outbreak diversity. *J. Theor. Biol.*, 232(1):71–81, <https://doi.org/10.1016/j.jtbi.2004.07.026> PMID: 15498594
6. Chowell G, Sattenspiel L, Bansal S, Viboud C (2016) Mathematical models to characterize early epidemic growth: A review. *Physics of Life Reviews*, 18:66–97, <https://doi.org/10.1016/j.plrev.2016.07.005> PMID: 27451336
7. Kim P, Lee CH (2018) Epidemic spreading in complex networks with resilient nodes: Applications to FMD. *Complexity*, 2018(5024327):9, <https://doi.org/10.1155/2018/5024327>
8. Herrera JL, Srinivasan R, Brownstein JS, Galvani AP, Meyers LA (2016) Disease Surveillance on Complex Social Networks. *PLoS Comput Biol* 12(7): e1004928. <https://doi.org/10.1371/journal.pcbi.1004928> PMID: 27415615
9. Bai Y, Yang B, Lin L, Herrera JL, Du Z, Holme P (2017) Optimizing sentinel surveillance in temporal network epidemiology. *Scientific Reports*, 7(4804), <https://doi.org/10.1038/s41598-017-03868-6>
10. Ames GM, George DB, Hampson CP, Kanarek AR, McBee CD, Lockwood DR, et al. (2011) Using network properties to predict disease dynamics on human contact networks. *Proc. R. Soc. B.*, 278:3544–3550, <http://doi.org/10.1098/rspb.2011.0290> PMID: 21525056
11. Cohen R, Havlin S, ben Avraham D (2003) Efficient immunization strategies for computer networks and populations. *Phys. Rev. Lett.*, 91:247901, <https://link.aps.org/doi/10.1103/PhysRevLett.91.247901> PMID: 14683159
12. Colman E, Holme P, Sayama H, Gershenson C (2019) Efficient sentinel surveillance strategies for preventing epidemics on networks. *PLoS Comput Biol* 15(11): e1007517. <https://doi.org/10.1371/journal.pcbi.1007517> PMID: 31765382
13. Schirdewahn F, Lentz HHK, Colizza V, Koher A, Hövel P, Vidondo B (2021) Early warning of infectious disease outbreaks on cattle-transport networks. *PLOS ONE*, 16(1):1–14, <https://doi.org/10.1371/journal.pone.0244999> PMID: 33406156
14. Holme P, Saramaki J (2012) Temporal networks. *Physics Reports*, 519(3):97–125, <https://doi.org/10.1016/j.physrep.2012.03.001>
15. Lloyd AL, May RM (2001). How viruses spread among computers and people. *Science*, 292(5520):1316–1317. <https://doi.org/10.1126/science.1061076> PMID: 11360990
16. Keeling MJ, Eames KT (2005) Networks and epidemic models. *J. R. Soc. Interface*, 2:295–307, <http://doi.org/10.1098/rsif.2005.0051> PMID: 16849187
17. Newman MEJ (2002b) Spread of epidemic disease on networks. *Phys. Rev. E*, 66:016128, <https://link.aps.org/doi/10.1103/PhysRevE.66.016128>
18. Rocha LEC, Masuda N (2016) Individual-based approach to epidemic processes on arbitrary dynamic contact networks. *Sci Rep* 6, 31456. <https://doi.org/10.1038/srep31456> PMID: 27562273
19. Karsai M, Perra N (2017) Control Strategies of Contagion Processes in Time-Varying Networks, pages 179–197. Springer Singapore, Singapore, [https://doi.org/10.1007/978-981-10-5287-3\\_8](https://doi.org/10.1007/978-981-10-5287-3_8).
20. Kao R, Danon L, Green D, Kiss I (2006) Demographic structure and pathogen dynamics on the network of livestock movements in great britain. *Proc. R. Soc. B*, 273:1999–2007, <http://doi.org/10.1098/rspb.2006.3505> PMID: 16846906
21. Gross T, D’Lima CJD, Blasius B (2006) Epidemic Dynamics on an Adaptive Network. *Phys. Rev. Lett.*, 96(20):208701. <https://doi.org/10.1103/PhysRevLett.96.208701> PMID: 16803215
22. Schwartz N, Cohen R, ben Avraham D, Barabási AL, Havlin S (2002) Percolation in directed scale-free networks. *Phys. Rev. E*, 66:015104. <https://doi.org/10.1103/PhysRevE.66.015104> PMID: 12241410
23. Allard A, Moore C, Scarpino SV, Althouse BM, Hébert-Dufresne L (2020) The role of directionality, heterogeneity and correlations in epidemic risk and spread. *arXiv:2005.11283* [Preprint]. 2020 [cited 2021]. Available from: <https://arxiv.org/abs/2005.11283>
24. Thurner S, Klimek P, Hanel R (2020) A network-based explanation of why most covid-19 infection curves are linear. *PNAS*, 117(37):22684–22689. <https://doi.org/10.1073/pnas.2010398117> PMID: 32839315
25. Vazquez F, Serrano M, Miguel M (2016) Rescue of endemic states in interconnected networks with adaptive coupling. *Scientific Reports*, 6(29342), <https://doi.org/10.1038/srep29342> PMID: 27380771
26. Rothenberg RB, Long DM, Sterk CE, Pach A, Potterat JJ, Muth S, et al. (2000) The Atlanta urban networks study: a blueprint for endemic transmission. *AIDS*, 14:2191–2200. <https://doi.org/10.1097/00002030-200009290-00016> PMID: 11061661



27. Eames KTD, Keeling MJ (2002) Modeling dynamic and network heterogeneities in the spread of sexually transmitted diseases. *PNAS*, 99(20):13330–13335. <https://doi.org/10.1073/pnas.202244299> PMID: 12271127
28. Ghani AC, Garnett GP (2000) Risks of acquiring and transmitting sexually transmitted diseases in sexual partner networks. *Sexually Transmitted Diseases*, 27:579–587. <https://doi.org/10.1097/00007435-200011000-00006> PMID: 11099073
29. Doherty IA, Padian NS, Marlow C, Aral SO (2005) Determinants and Consequences of Sexual Networks as They Affect the Spread of Sexually Transmitted Infections. *The Journal of Infectious Diseases*, 191(Supplement 1):S42–S54. <https://doi.org/10.1086/425277> PMID: 15627230
30. Eames KTD, Keeling MJ (2004) Monogamous networks and the spread of sexually transmitted diseases. *Mathematical Biosciences*, 189(2):115–130. <https://doi.org/10.1016/j.mbs.2004.02.003> PMID: 15094315
31. Pastor-Satorras R, Vespignani A (2001) Epidemic dynamics and endemic states in complex networks. *Phys. Rev. E*, 63:066117. <https://doi.org/10.1103/PhysRevE.63.066117> PMID: 11415183
32. Rothenberg R (2009) HIV transmission networks. *Current opinion in HIV and AIDS*, 4(4):260–265. <https://doi.org/10.1097/COH.0b013e32832c7cfc> PMID: 19532062
33. Sloot PM, Ivanov SV, Boukhanovsky AV, van de Vijver DA, Boucher CA (2008) Stochastic simulation of HIV population dynamics through complex network modelling. *International Journal of Computer Mathematics*, 85:8, 1175–1187. <https://doi.org/10.1080/00207160701750583>
34. Ferrari MJ, Bansal S, Meyers LA, Bjørnstad O (2006) Network frailty and the geometry of herd immunity. *Proc. R. Soc. B*. 2743–2748. <https://doi.org/10.1098/rspb.2006.3636> PMID: 17015324
35. Machado G, Galvis JA, Lopes FPN, Voges J, Medeiros AAR, Cárdenas NC (2020) Quantifying the dynamics of pig movements improves targeted disease surveillance and control plans. *Transbound. Emerg. Dis.* 2021; 68: 1663–1675. <https://doi.org/10.1111/tbed.13841> PMID: 32965771
36. Lentz HHK, Koher A, Hövel P, Gethmann J, Sauter-Louis C, Selhorst T, Conraths FJ (2016) Disease spread through animal movements: A static and temporal network analysis of pig trade in germany. *PLOS ONE*, 11(5):1–32. <https://doi.org/10.1371/journal.pone.0155196> PMID: 27152712
37. Valerio VC, Walther OJ, Eilittä M, Cissé B, Muneeppeerakul R, Kiker GA (2020) Network analysis of regional livestock trade in West Africa. *PLoS ONE* 15(5): e0232681. <https://doi.org/10.1371/journal.pone.0232681> PMID: 32407336
38. Kiss IZ, Green DM, Kao RR (2006) The network of sheep movements within great britain: network properties and their implications for infectious disease spread. *J. R. Soc. Interface*, 3:669–677. <http://doi.org/10.1098/rsif.2006.0129> PMID: 16971335
39. Kaluza P, Kölzsch A, Gastner M, Blasius B (2010) The complex network of global cargo ship movements. *J. R. Soc. Interface*, 7:1093–1103. <http://doi.org/10.1098/rsif.2009.0495> PMID: 20086053
40. Sterchi M, Faverjon C, Sarasua C, Vargas ME, Berezowski J, Bernstein A, et al. (2019) The pig transport network in Switzerland: Structure, patterns, and implications for the transmission of infectious diseases between animal holdings. *PLoS ONE*, 14(5). <https://doi.org/10.1371/journal.pone.0217974> PMID: 31150524
41. Kao RR, Green DM, Johnson J, Kiss IZ (2007) Disease dynamics over very different time-scales: foot-and-mouth disease and scrapie on the network of livestock movements in the UK. *J. R. Soc. Interface* 4907–916 <https://doi.org/10.1098/rsif.2007.1129>
42. Danon L, Ford AP, House T, Jewell CP, Keeling MJ, Roberts GO, et al. (2011) Networks and the epidemiology of infectious disease. *Interdiscip. Perspect. Infect. Dis.* 2011, 284909. <https://doi.org/10.1155/2011/284909> PMID: 21437001
43. Gorsich EE, Luis AD, Buhnerkempe MG, Grear DA, Portacci K, Miller RS, et al. (2016) Mapping U.S. cattle shipment networks: Spatial and temporal patterns of trade communities from 2009 to 2011. *Prev. Vet. Med.*, 134, p.82–91. <https://doi.org/10.1016/j.prevetmed.2016.09.023> PMID: 27836049
44. Silk MJ, Croft DP, Delahay RJ, Hodgson DJ, Boots M, Weber N, et al. Using Social Network Measures in Wildlife Disease Ecology, Epidemiology, and Management. *Bioscience*. 2017; 67:245–57. <https://doi.org/10.1093/biosci/biw175> PMID: 28596616
45. Mohr S, Deason M, Churakov M, Doherty T, Kao RR (2018) Manipulation of contact network structure and the impact on foot-and-mouth disease transmission. *Prev. Vet. Med.* 157, 8–18. <https://doi.org/10.1016/j.prevetmed.2018.05.006> PMID: 30086853
46. Pozo P, VanderWaal K, Grau A, de la Cruz ML, Nacar J, Bezos J, et al. (2019) Analysis of the cattle movement network and its association with the risk of bovine tuberculosis at the farm level in Castilla y Leon, Spain. *Transbound Emerg Dis.*; 66: 327–340. <https://doi.org/10.1111/tbed.13025> PMID: 30270505

47. Ortiz-Pelaez A, Pfeiffer D, Soares-Magalhães R, Guitian F (2006) Use of social network analysis to characterize the pattern of animal movements in the initial phases of the 2001 foot and mouth disease (fmd) epidemic in the UK. *Prev Vet Med*, 76:40–55. <https://doi.org/10.1016/j.prevetmed.2006.04.007> PMID: 16769142
48. Haydon D, Kao R, Kitching R (2004) The UK foot-and-mouth disease outbreak—the aftermath. *Nat Rev Microbiol* 2, 675–681. <https://doi.org/10.1038/nrmicro960> PMID: 15263902
49. Hayama Y, Firestone SM, Stevenson MA, Yamamoto T, Nishi T, Shimizu Y, et al. (2019) Reconstructing a transmission network and identifying risk factors of secondary transmissions in the 2010 foot-and-mouth disease outbreak in Japan. *Transbound Emerg Dis* 66:2074–2086, <https://doi.org/10.1111/tbed.13256> PMID: 31131968
50. Keeling MJ, Woolhouse ME, Shaw DJ, Matthews L, Chase-Topping M, Haydon DT, et al. (2001) Dynamics of the 2001 UK foot and mouth epidemic: stochastic dispersal in a heterogeneous landscape. *Science*. 2001 Oct 26; 294(5543):813–7. <https://doi.org/10.1126/science.1065973> PMID: 11679661
51. Tildesley MJ, Brand S, Brooks-Pollock E, Bradbury NV, Werkman M, Keeling MJ (2019) The role of movement restrictions in limiting the economic impact of livestock infections. *Nat Sustain* 2, 834–840 <https://doi.org/10.1038/s41893-019-0356-5> PMID: 31535037
52. Guyver-Fletcher G, Gorsich EE, Tildesley MJ (2021) A model exploration of carrier and movement transmissions potential explanatory cause for persistence of foot-and-mouth disease in endemic regions. *Transbound Emerg Dis*, 1–15. <https://doi.org/10.1111/tbed.14423>
53. Dawson PM, Werkman M, Brooks-Pollock E, Tildesley MJ (2015) Epidemic predictions in an imperfect world: modeling disease spread with partial data *Proc. R. Soc. B.* 282:20150205. <https://doi.org/10.1098/rspb.2015.0205> PMID: 25948687
54. Andel MV, Tildesley MJ, Gates MC (2021) Challenges and opportunities for using national animal datasets to support foot-and-mouth disease control. *Transbound Emerg Dis.*; 68:1800–1813. <https://doi.org/10.1111/tbed.13858> PMID: 32986919
55. Dawson PM (2016) On the analysis of livestock networks and the modelling of foot-and-mouth disease. PhD thesis, Centre for Complexity Science. The University of Warwick.
56. Buhnerkempe MG, Tildesley MJ, Lindström T, Grear DA, Portacci K, Miller RS, et al. (2014) The Impact of Movements and Animal Density on Continental Scale Cattle Disease Outbreaks in the United States. *PLoS ONE* 9(3): e91724. <https://doi.org/10.1371/journal.pone.0091724> PMID: 24670977
57. Barrat A, Barthélemy M, Pastor-Satorras R, Vespignani A (2004) The architecture of complex weighted networks. *Proceedings of the National Academy of Sciences*, 101(11):3747–3752. <https://doi.org/10.1073/pnas.0400087101> PMID: 15007165
58. Kitsak M, Gallos LK, Havlin S, Liljeros F, Muchnik L, Stanley HE, et al. (2010) Identification of influential spreaders in complex networks. *Nature Physics*, 6:888–893, <https://doi.org/10.1038/nphys1746>
59. Carmi S, Havlin S, Kirkpatrick S, Shavitt Y, Shir E (2007) A model of internet topology using k-shell decomposition. *Proceedings of the National Academy of Sciences*, 104(27):11150–11154, <https://doi.org/10.1073/pnas.070117510>
60. Batagelj V, Zaversnik M (2011) An o(m) algorithm for cores decomposition of networks. *Advances in Data Analysis and Classification*. Vol 5, 2, 129–145.
61. Newman MEJ (2010) *Networks: An Introduction*. Oxford University Press, 1st edition.
62. Newman MEJ, Strogatz SH, Watts DJ (2001) Random graphs with arbitrary degree distributions and their applications. *Phys. Rev. E*, 64:026118, <https://doi.org/10.1103/PhysRevE.64.026118> PMID: 11497662
63. Makarov VV, Kirsanov DV, Frolov NS, Maksimenko VA, Li X, Wang Z, et al. (2018) Assortative mixing in spatially-extended networks. *Scientific Reports*, 8(13825), <https://doi.org/10.1038/s41598-018-32160-4> PMID: 30218078
64. Newman MEJ (2002a) Assortative mixing in networks. *Phys. Rev. Lett.*, 89:208701, <https://link.aps.org/doi/10.1103/PhysRevLett.89.208701>
65. Wang Y, Chakrabarti D, Wang C, Faloutsos C (2003) Epidemic spreading in real networks: an eigenvalue viewpoint. In *22nd International Symposium on Reliable Distributed Systems*, 2003. *Proceedings.*, pages 25–34.
66. Blondel VD, Guillaume JL, Lambiotte R, Lefebvre E (2008) Fast unfolding of communities in large networks. *J. Stat. Mech. Theory Exp.* 2008, P10008 (2008). <https://doi.org/10.1088/1742-5468/2008/10/p10008>
67. Dugué N, Labatut V, Perez A (2015) A community role approach to assess social capitalists visibility in the Twitter network. *Social Network Analysis and Mining*, Springer, 5, pp.26.

68. Opsahl T, Colizza V, Panzarasa P, Ramasco JJ (2008). Prominence and control: The weighted rich-club effect. *Phys. Rev. Lett.*, 101:168702, <https://link.aps.org/doi/10.1103/PhysRevLett.101.168702> PMID: 18999722
69. Opsahl T, Panzarasa P (2009) Clustering in weighted networks, *Social Networks*, Volume 31, Issue 2, Pages 155-163, ISSN 0378-8733.
70. Opsahl T, Agneessens F, Skvoretz J (2010) Node centrality in weighted networks: Generalizing degree and shortest paths. *Social Networks*, Volume 32, Issue 3, Pages 245-251, ISSN 0378-8733, <https://doi.org/10.1016/j.socnet.2010.03.006>.
71. Csardi G, Nepusz T (2006) The igraph software package for complex network research. *InterJournal, Complex Systems*: 1695, <http://igraph.sf.net>.
72. Barthélemy M (2011) Spatial Networks. *Physics Reports*, Volume 499, Issues 1-3, Pages 1-101.
73. Sah P, Leu ST, Cross PC, Hudson PJ, Bansal S (2017) Unraveling the disease consequences and mechanisms of modular structure in animal social networks. *Proceedings of the National Academy of Sciences*, 114(16):4165–4170, ISSN:0027-8424, <https://www.pnas.org/content/114/16/4165> PMID: 28373567
74. Gross B, Havlin S (2020) Epidemic spreading and control strategies in spatial modular network. *Appl Netw Sci*, 5(95), <https://doi.org/10.1007/s41109-020-00337-4> PMID: 33263074
75. Cerqueti R, Ciciretti R, Dalò A, Nicolosi M (2022) A new measure of the resilience for networks of funds with applications to socially responsible investments, *Physica A: Statistical Mechanics and its Applications*, Volume 593, 126976, ISSN 0378-4371, <https://doi.org/10.1016/j.physa.2022.126976>.
76. Liu Y, Wang J, He H, Huang G, Shi W (2021) Identifying important nodes affecting network security in complex networks. *International Journal of Distributed Sensor Networks*.
77. Martinetti D, Soubeyrand S (2019) Identifying Lookouts for Epidemic-Surveillance: Application to the Emergence of *Xylella fastidiosa* in France. *Phytopathology* 109:2, 265–276. <https://doi.org/10.1094/PHYTO-07-18-0237-FI>
78. Ciaperoni M, Galimberti E, Bonchi F, Catutto C, Gullo F, Barrat A (2020) Relevance of temporal cores for epidemic spread in temporal networks. *Sci Rep* 10, 12529. <https://doi.org/10.1038/s41598-020-69464-3> PMID: 32719352
79. Mastin AJ, Gottwald TR, van den Bosch F, Cunniffe NJ, Parnell S (2020) Optimising risk-based surveillance for early detection of invasive plant pathogens. *PLoS Biol* 18(10): e3000863. <https://doi.org/10.1371/journal.pbio.3000863> PMID: 33044954
80. Menichetti G, Remondini D, Panzarasa P, Mondragón RJ, Bianconi G (2014) Weighted Multiplex Networks. *PLoS ONE* 9(6): e97857. <https://doi.org/10.1371/journal.pone.0097857> PMID: 24906003